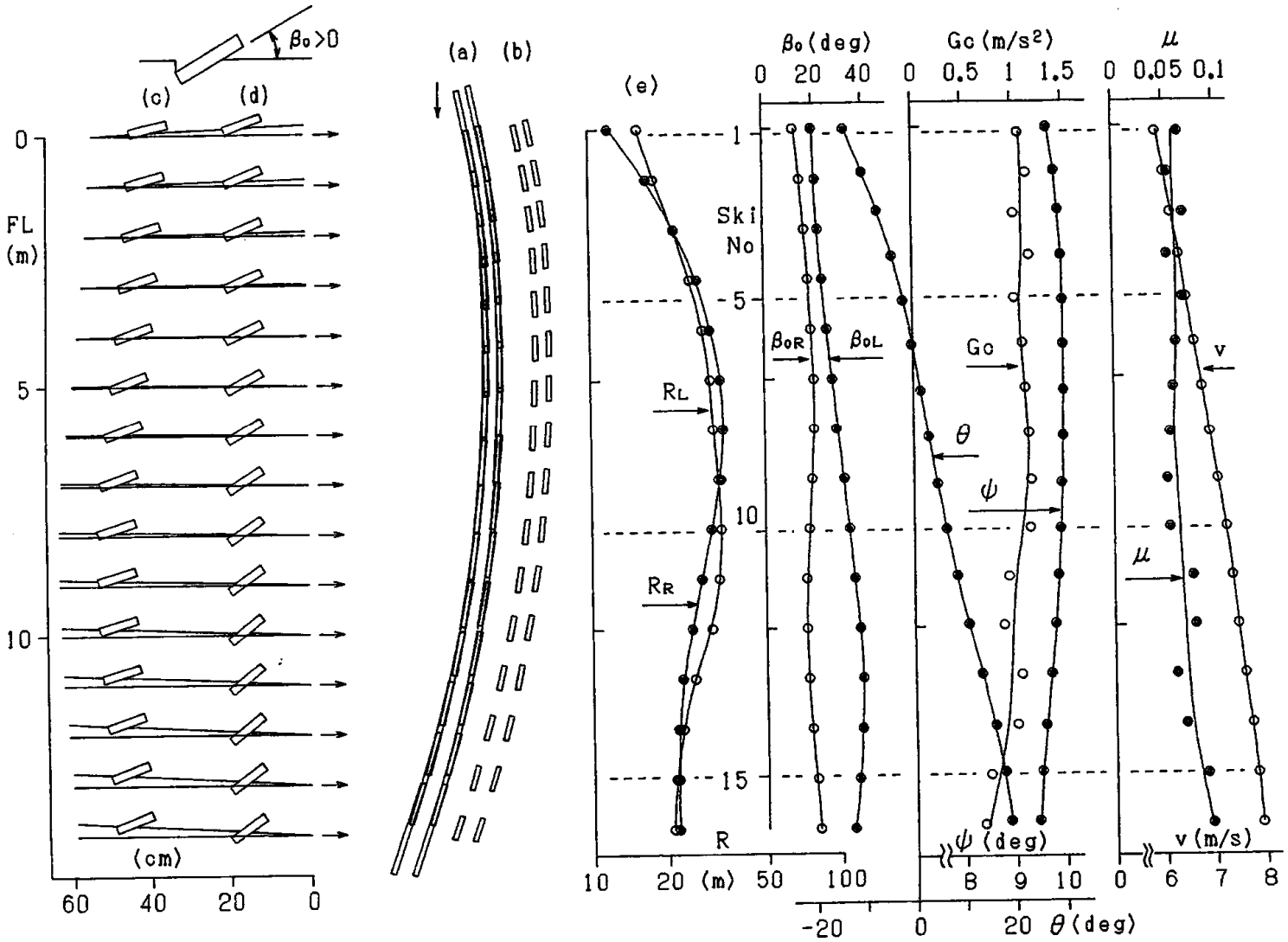

Figure 6 Analysis of carving turns using conventional skis. R, β_1, β_O, θ, ψ, G_C, v and μ are the same as in Fig. 5.

The skidding angle was almost the same for carving skis and conventional skis. However, the values of R, G_C and μ were different for the two ski types.

Parallel turn using conventional skis

Figure 7 shows the schemata obtained by reanalysing the data in the paper by Sahashi & Ichino (1996). The skis numbered 1–7 indicate straight downhill runs. The skis numbered 8–13 indicate a carving turn, which leaves a much clearer ski track on the snow plane as there is less skidding. For the skis numbered 1–13, the edging angle β_O was measured from the mark of the sliding track. For number 14 and above, there was considerable skidding such that no track appeared on the snow plane, therefore β_O could not be measured. However, we estimate β_O for a parallel turn with the ski positions numbered 14 and above to be approximately $\pm$ 10° from β_O for positions 1–13.

During the descent shown in Fig. 7, the ski angle of both skis was almost equal. Let δ represent this angle; $\delta \approx$ tangential angle θ for ski numbers 1–13 with less skidding. In contrast, for the high-skid condition of skis numbered 14 and above, $|\delta| > |\theta|$. Table 1 shows these values.

Ski width and radius of curvature of side-cut

Figure 8(a) shows the measured values regarding the width of the carving skis and conventional skis, which were used in the experiments. The ski boots are mounted on the skis at the point of minimum

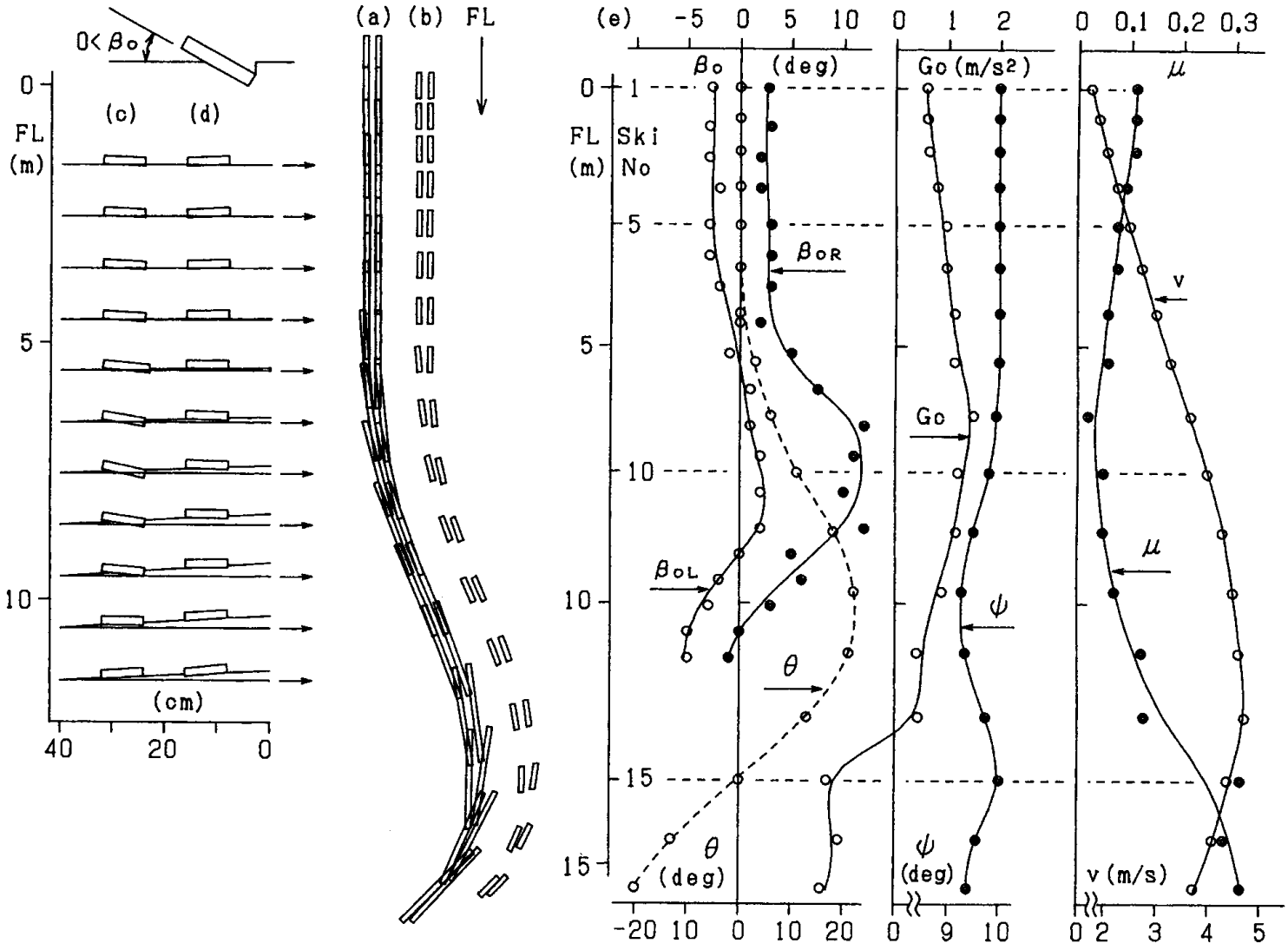

Figure 7 Analysis of parallel turns using conventional skis. R, β_1, β_O, θ, ψ, G_C, v and μ are the same as in Fig. 5.

Table 1 Ski angle δ and tangential angle θ of parallel turns by conventional skis shown in Fig. 7

Ski number	Tangential angle θ	Ski angle δ_R	Ski angle δ_L
13	21°	21°	20°
14	13°	10°	8°
15	0°	−1°	−8°
16	−17°	−24°	−27°
17	−20°	−45°	−43°

width. The carving skis and the conventional skis have similar widths at the boot-mounting position, whereas carving skis are wider than conventional skis at the ski tip and tail. Figure 8(b) shows the radius of curvature of the side-cut of each ski. We can see that the curvature is not even and is relatively large at the boot-mounting position. Overall, the radius of curvature is between 10 and 20 m for carving skis and never less than 20 m for conventional skis.

Curvature variation of side-cut with edging

The radius of curvature of the side-cut, R_1 of carving skis used in Fig. 5 is irregular and varies in the range of 10–20 m, as shown in Fig. 8. However, let us assume that the radius is fixed ($R_1 = 15$ m). The length of the region shaped like a reel, as shown in Fig. 4(a), is shorter than the total length of the ski. Given that the length of the reel-shaped region of the carving ski is $SL = 1.6$ m, the half-angle of the arc is represented by $\xi_1 = 3.1°$, as derived from Eq. (1).

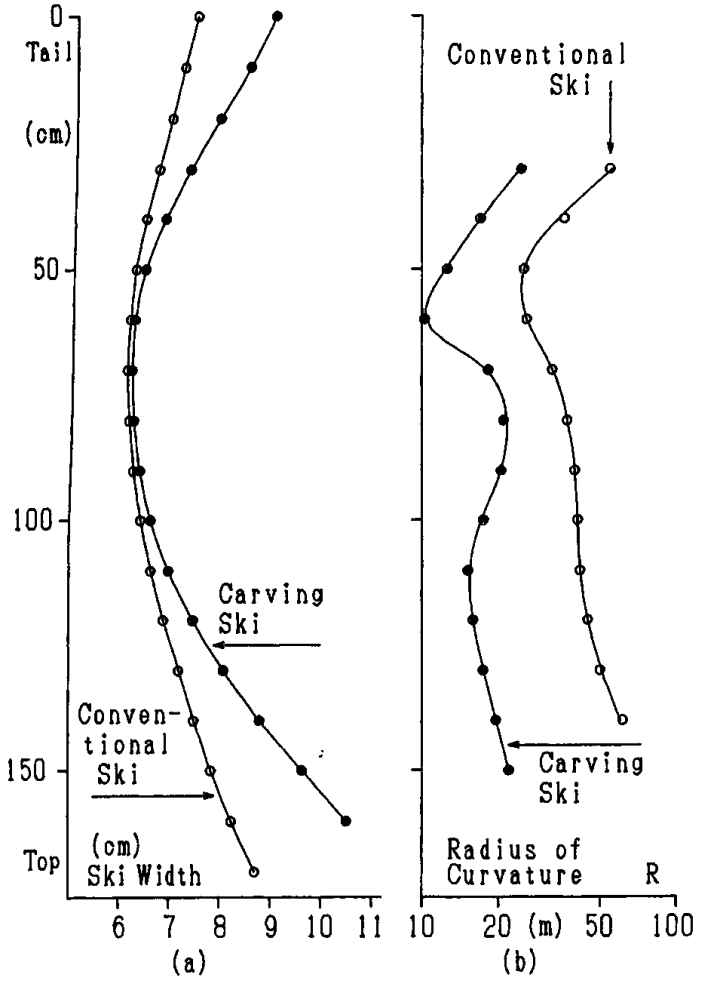

Figure 8 Analysis of the external form of carving skis and conventional skis. (a) Ski length and width. (b) Radius of curvature of side-cut.

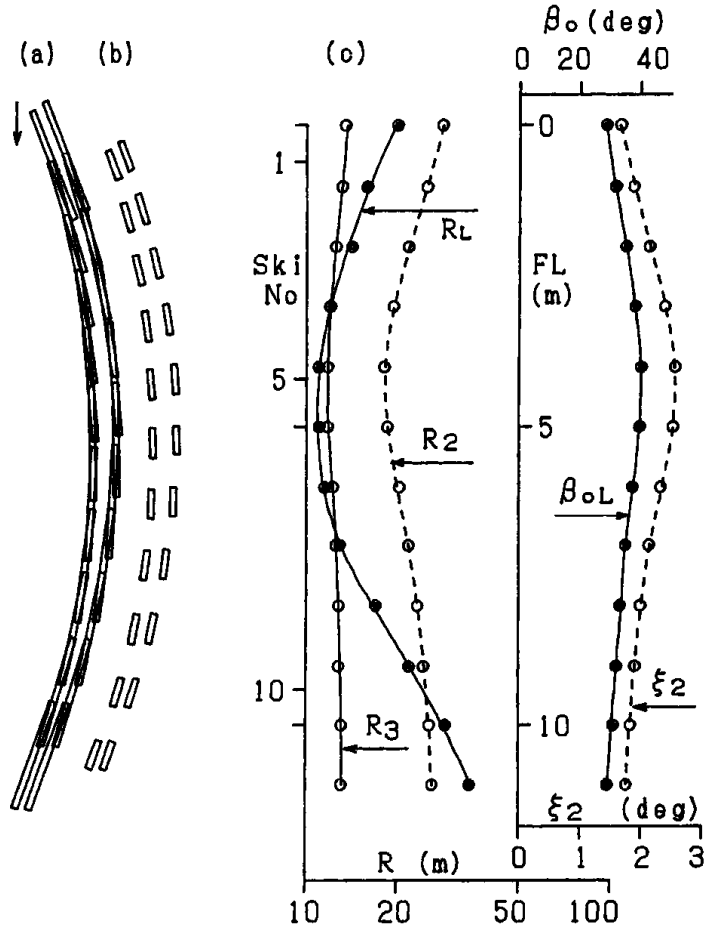

Figure 9 The change of the radius of curvature R_3 of side-cut depending on edging angle. (a) and (b) The same ski loci as in Fig. 5. (c) The solid lines indicate the curvature R_3. The dotted line R_2 indicates the radius of the cylinder in Fig. 4(b). ξ_2 is the angle in Fig. 4(c). β_{OL} and R_L are copied from Fig. 5(e).

Suppose that a skier is skiing with an edging angle β_{OL} of the left ski (outside ski).

Then β_{OL} is equal to β_O. When the snow plane is assumed to be a horizontal plane, then β_{OL} is equal to β. When β_{OL} undergoes changes like those shown in Fig. 5(e), we assume that the radius of curvature of the descent ski track becomes R_3, which was obtained in the cylinder approximation. In Fig. 9, ξ_2 and R_2 were derived from Eqs (2) and (3) by setting $\beta = \beta_{OL}$, and R_3 was derived from Eqs (4) and (5). Figure 9(a), (b), R_L and β_{OL} are the same as those in Fig. 5. As shown in Fig. 9, R_3 is almost constant (13 m). For ski numbers 3–8, it can be said that R_3 almost equals R_L and the cylinder approximation holds. That is, a ski having a side-cut with a radius R_1 slides with an edging angle β_{OL} on a circle track with radius R_3. The half-angle of the central angle forming the arc of radius R_3 was $\xi_3 = 3.6°$. The radius of the cylinder, R_2, was almost twice R_3. ξ_2 was half of ξ_3. However, we consider that the cylinder approximation does not hold when $R_3 \neq R_L$.

In accordance with the cylinder approximation, we studied the effect of varying the edging angle β on the values of R_2 and R_3 (Fig. 10). The solid lines indicate R_2 and R_3 when $SL = 1.6$ m and $R_1 = 10$ m, assuming carving skis. Within the range of $14° < \beta < 78°$, the assumption that the ski surface forms a part of a cylinder surface holds, that is, $C_2' = C_2$. When β is narrow, $R_3 \approx R_1$ holds. As β becomes wider, R_3 becomes shorter than R_1. When $14° > \beta$, the shovel of the ski rises up from the snow plane and becomes $C_2' < C_2$, if the cylinder approximation must be satisfied. On the other hand, if the

intention is to keep $C_2' = C_2$, then the cylinder approximation will not hold. When $78° < \beta$, C_2' is longer than C_2 and again the cylinder approximation will not hold. The dotted lines shown in Fig. 10 indicate R_2 and R_3 when $SL = 1.6$ m and $R_1 = 30$ m, assuming conventional skis.

Discussion

Comparison with carving turn and parallel turn

The coefficient of kinetic friction μ for the carving turn shown in Fig. 5(e) is almost constant and is unrelated to the turning direction. The ski acceleration, G_C, is positive. In Fig. 7, μ is almost constant and G_C is positive for ski numbers 1–11, indicating a straight downhill run and carving turns. When the skis begin turning in the direction of the FL (ski numbers 14–17), both the skidding of the skis and μ become greater and G_C becomes negative. This indicates that skis exhibit accelerated sliding with less skidding and decelerated sliding with more skidding.

For carving turns, the skidding shown in Figs 5 and 6 is approximately 1°, and for ski numbers 8–11 in Fig. 7 it is approximately 2°. In contrast, for parallel turns, the skidding for ski numbers 15–17 in Fig. 7 is approximately 20°.

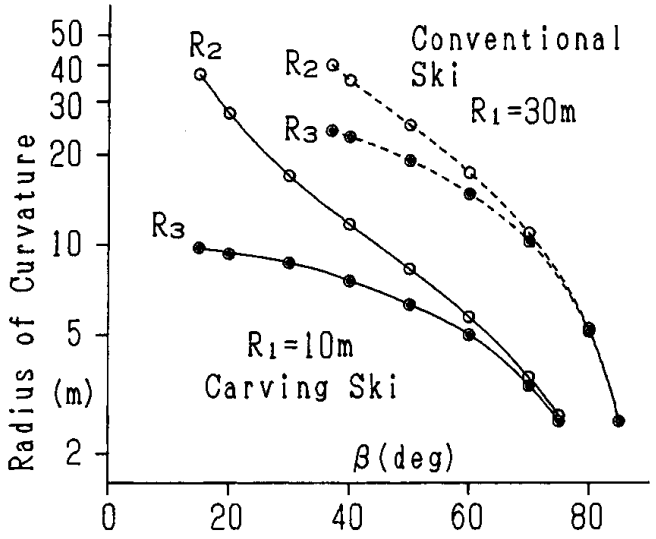

Figure 10 The radius of curvature R_3 of side cut and the radius R_2 of the cylinder. The solid lines correspond to carving skis, and the dotted line corresponds to conventional skis.

Relation between ski angle δ and tangential angle θ

Figure 11(a) schematically shows skis with a length of 180 cm and a width of 20 cm on an arc with a radius of 6 m. In Fig. 11(a)-3, the ski angle δ equals the tangential angle θ; that is, $\delta = \theta$. Hence, an arc with a radius of 6 m that passes through a corner of one ski passes through the corners of all other skis. In Fig. 11(a)-1, δ is greater than θ by 20°, which is similar to the parallel turn within the range of ski numbers 16–17 in Fig. 7. This part of the descent is a turning descent with wide skidding. For the parallel turn measured by Sahashi & Ichino (1998), the skidding was approximately 20° when the radius of the track was 6 m; this bears a close resemblance to the schema shown in Fig. 11(a)-1. Based on our measurement, one of the features of the turning descent with wide skidding is that the ski tails skid to the outer side of the turning track. The dotted lines shown in Fig. 11(a)-1, -2 and -4 describe the arcs passing through the midpoints of the skis. Each position in Fig. 11(a)-2 and -4 is described with $\delta = \theta \pm 10°$. In our experiments, we

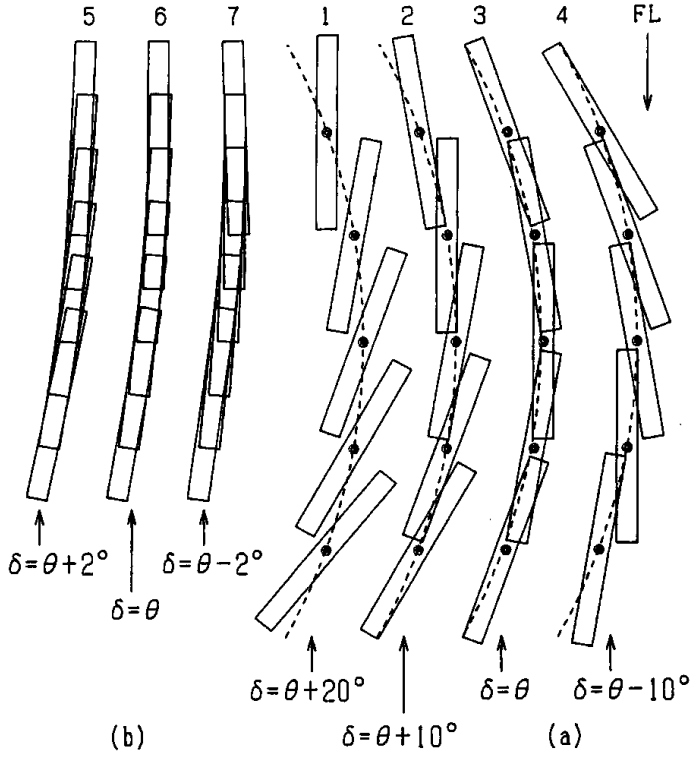

Figure 11 (a) Skis placed on arcs having a track radius of 6 m (b) Skis placed on arcs having a track radius of 15 m. δ is the ski angle and θ is the tangential angle.

have not observed a descent which is marked by wide skidding in which the ski tips skid to the outer side of the turning track [shown in Fig. 11(a)-4].

Figure 11(b) illustrates skis which are on circular tracks with a radius of 15 m. In Fig. 11(b)-6, $\delta = \theta$ and the skis are described with $\delta = \theta \pm 2°$ in each of Fig. 11(b)-5 and (b)-7. For the carving turn shown in Figs 5 and 6, either the ski tails or the ski tips skid outward from the descent track. This skidding in the carving turn is approximately $\pm$ 1°; accordingly, we can see that the carving turns in Figs 5 and 6 bear a close resemblance to the schemata indicated in Fig. 11(b).

Edging angle and side-cut It has been said by Evans *et al.* (1974) and Maruyama *et al.* (1994) that turning is caused by the side-cut, whereby the skis slide along the arc of the side-cut according to the edging angle. Using the edging angle that we measured, we studied the change of the arcs formed by a side-cut, based on the cylinder approximation. R_3 indicated in Fig. 9(c) was obtained as a result. However, comparing this value of R_3 with the radius of curvature R_L derived from the ski locus, we see not only some resemblances but also some differences between them. This appears to indicate that ski tracks depend on factors other than arcs formed by side-cuts.

Carving turn and skidding If the side-cut has a specific radius, then skis can be described on a track having a specific radius, as indicated in Fig. 11(a)-3. This figure corresponds to a turning descent without skidding. However, the side-cut radius of curvature (Fig. 8) and the radius of tracks (Fig. 5) are both irregular. Hence, we infer that an accumulation of slight skidding leads to the experimentally derived carving turn. The carving turn seems to be defined not as a turning descent without skidding, but as a turning descent in which the ski angle θ and the tangential angle δ are almost equal.

On the other hand, the conventional parallel turn becomes a turning descent with more skidding.

Conclusions

We have described our experiments of carving turns performed with both carving skis and conventional skis. The experiments revealed that turning descents with a smaller coefficient of kinetic friction and less skidding are possible in carving turns as compared to conventional parallel turns. However, the cause of carving turns seems to be difficult to explain with the side-cut of skis edged at an angle to the snow plane. Consequently, it is concluded that the carving turn descent is defined as one that satisfies $\theta = \delta$.

Acknowledgements

The authors would like thank Mr Kamihira in the Hohnoki-Daira Ski Are, Gifu Prefecture, for the experiments on snow.

References

Evans, H., Jackman, B. & Otlaway, M. (1974) *We Learned to Ski*. New York, NY, USA. St Martin's Press.

Ichino, S. (1999). Revolution in ski: carving technique. *Ski Journal*, Ski Journal Co., Ltd., Tokyo, Japan. [in Japanese].

Maruyama, S., Okuda, E., Watanabe, S., Hirakawa, H., Masuda, C., Murasato, T. & Suzuki, S. (1994) Japan Ski Kyotei (The Text of Ski Association of Japan). *Ski Journal*, Ski Journal Co., Ltd., Tokyo, Japan. [in Japanese].

Sahashi, T. & Ichino, S. (1990) Experimental study of the mechanism of skiing turns. II. Measurement of edging angles. *Japanese Journal of Applied Physics*, **29**, 1203–1208.

Sahashi, T. & Ichino, S. (1995) Method for drawing locus of a sliding ski as observed from direction perpendicular to snow surface. *Japanese Journal of Applied Physics*, **34**, 674–679.

Sahashi, T. & Ichino, S. (1996) Experimental study of the mechanism of skiing turns. III. Measurement of edging angles of skis on snow. *Japanese Journal of Applied Physics*, **35**, 2377–2382.

Sahashi, T. & Ichino, S. (1998) Coefficient of kinetic friction of snow skis during turning descents. *Japanese Journal of Applied Physics*, **37**, 720–727.